

Nonlinear modeling of the photon pair generation in ring resonators

A. FAZACAS^{a,b}, P. STERIAN^{a,c}

^aAcademic Center for Optical Engineering and Photonics, Faculty of Applied Sciences, University "Politehnica" of Bucharest, 313 Splaiul Independentei, 060042 Bucharest, Romania;

^bInstitute of Atomic Physics, Bucharest, Romania

^cAcademy of Romanian Scientists, 54 Splaiul Independentei, 050094 Bucharest, Romania

Nonlinear optical effects in silicon micro-structures were studied in recent years. In this paper we studied the Kerr nonlinear effects in silicon-on-insulator (SOI) micro ring resonator in order to generate quantum-correlated photon pairs. To achieve this objective we used the four-wave mixing phenomenon (FWM), that occurs when two or more different wavelengths are released into optical fibers. By using continuous wave (CW) power pumps we demonstrate the photon pair generation in a 40 μm SOI ring resonator. Photon pair generation play an important role in quantum communication at 1.5 μm telecommunication wavelength. Also, the entangled photons can be used to in quantum cryptography, to encode or decode signals, or in entanglement-assisted teleportation. SOI chips can also be used, in future, for acceleration of charged particles in optical photonic structures. In our simulations we used The Finite Difference Time-Domain Method (FDTD), a powerful mathematical tool to solve Maxwell equations in micro-structures.

(Received June 25, 2014; accepted May 7, 2015)

Keywords: Micro-ring resonators, Photon pair, Four-wave mixing, Entanglement, Nonlinear effects, SOI, FDTD

1. Introduction

Silicon-on-insulator (SOI) technology was used in the last years due to the need to extend Moore's Law, but also due to the remarkable proprieties of this type of material, namely: low parasitic capacitance, high refractive index, low passive current, nonlinearity, and resistance to latchup. These proprieties make silicon-on-insulator attractive for optical waveguides and other passive optical devices. Another advantage of SOI is the low manufacturing price [1-8].

Silicon-on-insulator chips were used demonstrate the acceleration of charged particles in optical photonic structures by using infrared lasers [9-11]. Nowadays, particle accelerators are huge and expensive, such as the Large Hadron Collider from CERN, the largest particle accelerator that lies in a tunnel of 27 kilometers buried underneath the border of France and Switzerland. Due to the maintenance high cost of particle accelerators, scientists from SLAC National Accelerator Laboratory try to shrink accelerators to the size of a microchip. They manage to design a woodpile photonic crystal accelerator with high coupling efficiencies. Consequently, by using high power lasers and silicon photonic structures/fibers could be used in future particle physics experiments with potential applications in portable particle accelerators and for the treatment of cancerous tumours [10-13].

In this paper we theoretically study the photon pair generation in SOI micro-ring resonators by using the four-wave mixing phenomena (FWM). FWM is a Kerr nonlinear effect that occurs due to the third-order susceptibility χ^3 when two or more different wavelengths are used in photonic devices. In their paper, Sharping et.

all described experimentally the generation of correlated photons in nanoscale silicon waveguides (using FWM) stating that their measurements are a first step towards the CMOS-SOI development of tools for quantum information processing [1]. Others described experimentally the photon pair production in SOI waveguides and in optical fibers [2-4]. Recent studies described the propagation of entangled photon-pairs in photonic crystals and in nonlinear microstructure optical fibers [5, 6]. Theoretical studies of FWM in silicon waveguides to generate correlated photon pairs were described by Q. Lin and Godvind P. Agrawal [7, 14-17]. Palmett et. all studied the generation of photon pairs by spontaneous FWM in photonic crystal optical fiber and showed that it is possible to design a source of entangled photon pairs with practical application in quantum information processing [8]. Another important result was obtained by Eli Megidish and Hagai Eisenberg who entangled two photons that don't exist at the same time, hoping that with this technique they will create quantum networks for the transmission of unbreakable communications [18-21]. By using stimulated emission to amplify photons pairs, Pavel Sekatski et all. have created multiphoton states that can be used in quantum information technology [19].

Micro-ring resonator consisting of a unidirectional coupling between a ring and a waveguide can be used in a variety of application ranging from filters [14] and sensing [15, 16] to quantum photon pair generation [16]. Photon pair generation or quantum entanglement is a physical phenomenon that occurs when a laser beam fired through a crystal generates a pair of photons that interact over long distances. Entanglement has many applications ranging from coding and teleportation to interferometry and

occurs, also, for direct interaction between other subatomic particles. I. McGregor and K. M. Hock described in their paper a novel particle accelerating structure made of split-ring resonators etched into a copper rectangular waveguide [22].

2. Theoretical background

Four-wave mixing is a nonlinear Kerr optical effect that occurs when the light of two or more wavelengths is released into an optical fiber, resulting in a new wavelength, also known as idler wavelength. For different types of input wavelengths the idler wavelength is described by the following equation:

$$\lambda_{idler} = \lambda_{i1} + \lambda_{i2} - \lambda_{signal} \quad (1)$$

If the input wavelengths are identical (as we see in Figure 1a) we are in the case of degenerated four-wave mixing (DFWM) and $\lambda_{i1} = \lambda_{i2}$. In degenerated four-wave mixing case three wavelengths are involved, namely: the input

wavelength, the idler wavelength and the signal wavelength [23].

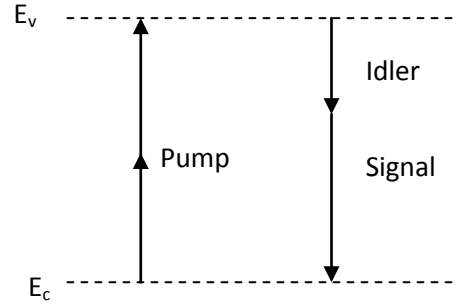


Fig. 1 Schematic view of the four-wave mixing phenomena in the case of two identical input wavelengths

To describe mathematically the FWM phenomena we assume that the three wavelengths mentioned above are in the following form:

$$A(z,t) = A_{pump}(z,t)e^{-i\omega_{pump}t} + A_{signal}(z,t)e^{-i\omega_{signal}t} + A_{idler}(z,t)e^{-i\omega_{idler}t} \quad (2)$$

In continuous wave regime if we assume that the free carrier life time are shorter than the field amplitudes [24],

the individual frequencies reduces to the following equations:

$$\frac{\partial A_p}{\partial z} = i\beta_p A_p + i\gamma_e |A_p|^2 A_p + i\gamma_f \tau_0 |A_p|^4 A_p \quad (3)$$

$$\frac{\partial A_s}{\partial z} = i\beta_s A_s + 2i\gamma_e |A_p|^2 A_s + i\gamma_e A_p^2 A_s^* + i\gamma_f \tau_0 |A_p|^2 \left[|A_p|^2 A_s + \frac{2}{1+i(\omega_p - \omega_s)\tau_0} (|A_p|^2 A_s + A_p^2 A_s^*) \right] \quad (4)$$

$$\frac{\partial A_i}{\partial z} = i\beta_i A_i + 2i\gamma_e |A_p|^2 A_i + i\gamma_e A_p^2 A_i^* + i\gamma_f \tau_0 |A_p|^2 \left[|A_p|^2 A_i + \frac{2}{1+i(\omega_p - \omega_i)\tau_0} (|A_p|^2 A_i + A_p^2 A_i^*) \right] \quad (5)$$

where

$\gamma_e = \gamma_0(\omega_0) + \frac{i}{2}\beta_T'(\omega_0)$ is the electronic nonlinear parameter with $\gamma_0 = \frac{\omega_0 n_2}{ca}$ nonlinear Kerr parameter;

$\beta_T' = \frac{\beta_T}{a}$ is the two photon absorption coefficient normalized by the effective mode area $\bar{a} = (a_i a_j a_k a_l)^{1/4}$ and

$$\gamma_f = \frac{\beta_T}{2\hbar\omega_0 a^2} \frac{n_0(\omega_0)}{n(\omega_0)} \left[\frac{\omega_0}{c} \sigma_n(\omega_0) + \frac{i}{2} \sigma_a(\omega_0) \right] \quad (6)$$

$$\sigma_n(\omega) = \frac{n_f}{N}; \sigma_a(\omega) = \frac{\alpha_f}{N}$$

where α_f governs free-carrier absorption and n_f is the free-carrier index, N is the free-carrier density [24].

The FDTD algorithm is described by the following system of six coupled scalar equations:

$$\frac{\partial \vec{H}_{x,y,z}}{\partial t} = -\frac{1}{\mu} \left[\frac{\partial E_{y,z,x}}{\partial z, x, y} - \frac{\partial E_{z,x,y}}{\partial y, z, x} - \vec{M}_{source_{x,y,z}} \right] \quad (7)$$

$$\frac{\partial \vec{E}_{x,y,z}}{\partial t} = \frac{1}{\epsilon} \left[\frac{\partial H_{z,x,y}}{\partial y, z, x} - \frac{\partial H_{y,z,x}}{\partial z, x, y} - \vec{J}_{source_{x,y,z}} \right]$$

where \vec{E} is the electric field (V/m), \vec{D} is the electric flux density (C/m²), \vec{H} is the magnetic field (A/m), \vec{B} is the magnetic flux density (Wb/m²), and \vec{J} is the electric current density (A/m²), ϵ (F/m), μ is the magnetic

permeability (H/m). \vec{J}_{source} and \vec{M}_{source} are written as:

$$\vec{J} = \vec{J}_{source} + \sigma \vec{E}; \quad \vec{M} = \vec{M}_{source} + \sigma^* \vec{H} \quad (8)$$

where σ is the electric conductivity (S/m) and σ^* is the magnetic loss (Ω/m) and are equal to zero in our case [25-29].

If we consider the bi-dimensional case when the photonic device is in the X-Z plane and the propagation is made along the Z axis and the Y axis is considered infinite, then the Maxwell equations derive into two sets of independent equation, namely transversal electric (TE) and transversal magnetic (TM) that are described in the Table 1[30,31].

Table 1. The two sets of independent equation, transversal electric (TE) and transversal magnetic (TM) derived from Maxwell equations.

Transversal electric	Transversal magnetic
The components of the field are $H_x, E_y, H_z \neq 0$ and the propagation is made along the z axis:	The components of the field are $E_x, H_y, E_z \neq 0$ and the propagation is made along the z axis:
$\frac{\partial E_y}{\partial t} = \frac{1}{\varepsilon} \left[\frac{\partial H_x}{\partial z} - \frac{\partial H_z}{\partial x} \right]$	$\frac{\partial H_y}{\partial t} = \frac{1}{\mu_0} \left[\frac{\partial E_x}{\partial z} - \frac{\partial E_z}{\partial x} \right]$
$\frac{\partial H_x}{\partial t} = \frac{1}{\mu_0} \frac{\partial E_y}{\partial z}$	$\frac{\partial E_x}{\partial t} = \frac{1}{\varepsilon} \frac{\partial H_y}{\partial z}$
$\frac{\partial H_z}{\partial t} = -\frac{1}{\mu_0} \frac{\partial E_y}{\partial x}$	$\frac{\partial E_z}{\partial t} = -\frac{1}{\varepsilon} \frac{\partial H_y}{\partial x}$

In Kerr media photon pair generation occurs the light of two or more wavelengths is released into a optical fiber, resulting a new wavelength. Photon pair spectral density flux in ring resonator is described by the following equation:

$$f = (F_p^2 F_s F_i \gamma P L_{ring}) \quad (9)$$

where $\gamma = \frac{2\pi n_2}{\lambda A_{eff}}$ is the nonlinear term, P is the power,

$L_{ring} = 2\pi r$ is the length of the ring, F_p is the enhancement field at the pump frequency, F_s is the enhancement field at the signal frequency, F_i is the enhancement field at the idler frequency [32]. The enhancement fields are:

$$F = \frac{T}{\left(\frac{T}{2} + \frac{\eta}{2}\right)^2 + 4 \sin^2 \frac{\phi}{2}} \quad (10)$$

where T is the intensity transmission coefficient of the coupler and η is the linear intensity losses within the ring, and $\phi = 2\frac{2\pi}{\lambda} n_{eff} L_{ring}$ is the accumulated phase during one round trip in the ring [32].

3. Numerical results in ring resonator

In our simulations we considered a micro-ring resonator as seen in Figure 2 with the effective refractive index equal to 3,03, the length of the ring to be equal to $L = 2\pi r = 12,56 \mu m$, and the length of the waveguide is $40 \mu m$.

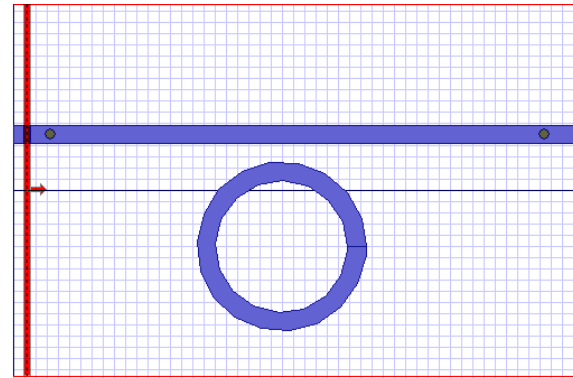


Fig. 2. Geometrical section of the micro-ring resonator with $r = 2 \mu m$

In order to obtain the theoretical evolution of the photon pair flux we considered that the transmission is equal to 1 and there are no linear losses in the ring. Consequently, the enhancement field becomes:

$$F = \frac{1}{\left(\frac{1}{2}\right)^2 + 4 \sin^2 \frac{\phi}{2}} \quad (11)$$

For different effective area of the waveguide we present, in Fig. 3, the evolution of the photon pair flux as evolution of pump power in micro-ring resonator. We can observe that the photon pair flux in micro-ring resonator increases with the increase of the pump power. Also, in a lower effective area of the waveguide, the photon pair flux increases. Experimentally, as described in [1, 32], the field enhancement factors decreases due to the losses in the ring.

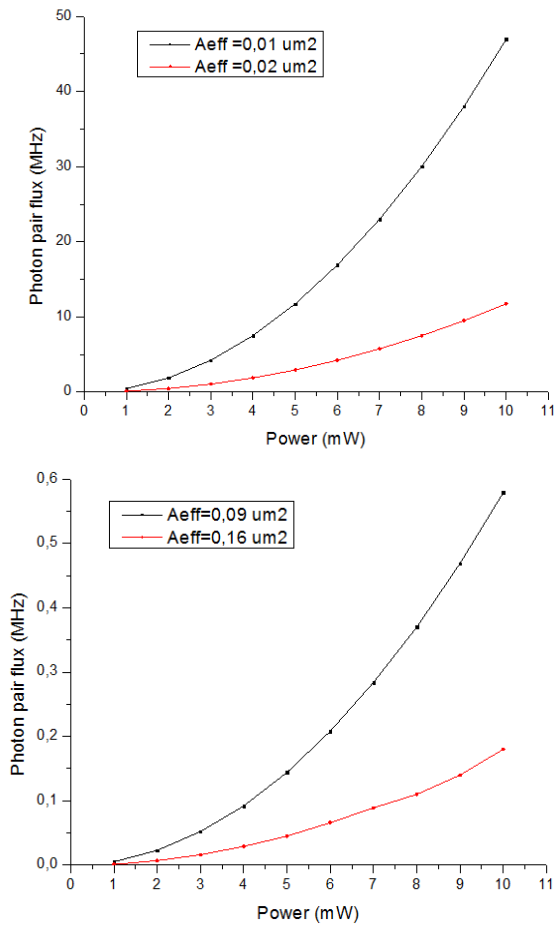


Fig. 3. The evolution of the photon pair flux as function of pump power in micro-ring resonator for different effective area of the waveguide

By using FDTD algorithm we simulated the evolution of two equal pump powers in micro-ring resonator, in continuous wave (CW) regime. For our simulation we considered that the relative linear permittivity is equal to 9,1809, the response time is equal to $5 \cdot 10^{-10}$ s and the permittivity is $6,58 \cdot 10^{-18}$ (m^2/V^2). The effective area of the waveguides were $0,01 \mu m^2$ and $0,09 \mu m^2$ and the identical simulation wavelengths were $1,5 \mu m$. In Figure 4 we can observe the evolution of the E_y component of the field as function of the propagation distance. In the first case, when the effective area of the waveguide was equal to $0,01 \mu m^2$, most of the signal remains in the waveguide. In the second case, when the effective area of the waveguide was equal to $0,09 \mu m^2$, the signal in the waveguide is lower and in the ring higher.

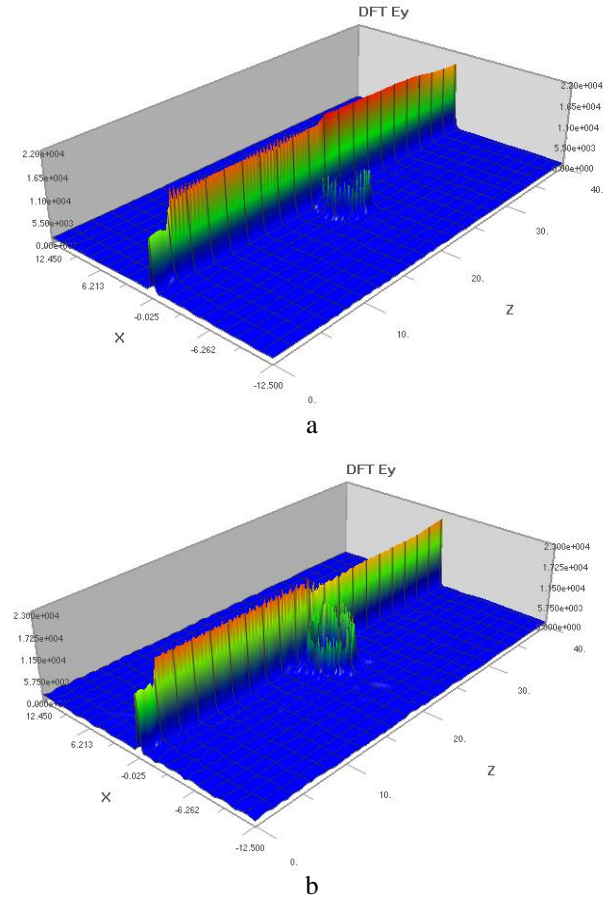


Fig. 4. The evolution of the E_y component of the field as function of the propagation distance for two identical pump powers and two effective area $0,01 \mu m^2$ (a) and $0,09 \mu m^2$ (b)

Using equation (1) and the results obtained from Fig. 5 we determine the idler frequencies for two pump wavelengths equal to $1,5 \mu m$ and pump power equal to $0,01 W/m$. The idler wavelength determined for the effective area of $0,01 \mu m^2$ (up) was equal to $1,686 \mu m$ and for the effective area of $0,09 \mu m^2$ (down) was equal to $1,688 \mu m$. The green line is the signal in a observation point situated at the input of the waveguide, while the brown line is the signal in a observation point situated at the output of the waveguide [32-37].

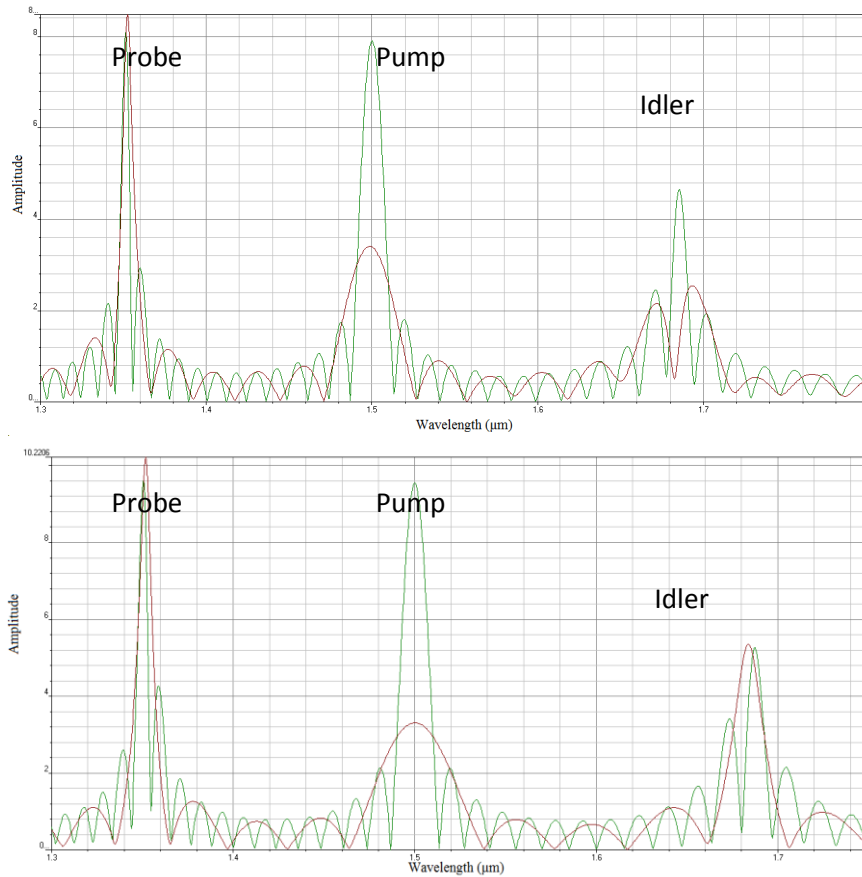


Fig. 5. The evolution of the optical field as function of wavelength for two identical pump powers and two effective area $0,01 \mu\text{m}^2$ (up) and $0,09 \mu\text{m}^2$ (down)

If we consider different input wavelengths $1,45 \mu\text{m}$ for the first input plane and $1,5 \mu\text{m}$ for the second input plane we can observe that the components of the electric field have a solitonic behaviour as seen in Figure 6. Also, we can observe that the signal is smoother than in the previous case and that the signal in the ring is much smaller than in the waveguide. For this simulation we considered same input powers and same effective areas of the waveguide as mentioned above

If the effective area of the waveguide is equal to $0,09 \mu\text{m}^2$ we can observe that the signal in the ring is higher than in the smaller waveguide. The idler wavelength determined for the effective area of $0,01 \mu\text{m}^2$ (up) was equal to $1,629 \mu\text{m}$ and for the effective area of $0,09 \mu\text{m}^2$ (down) was equal to $1,636 \mu\text{m}$.

In both cases (two identical pump powers and different pump powers) we can observe that for our micro-ring can output approximately 17 pairwise-correlated peaks situated between $1,2 \mu\text{m}$ and $1,8 \mu\text{m}$. Also, we can observe that for broader waveguides the amplitude of the signal is higher.

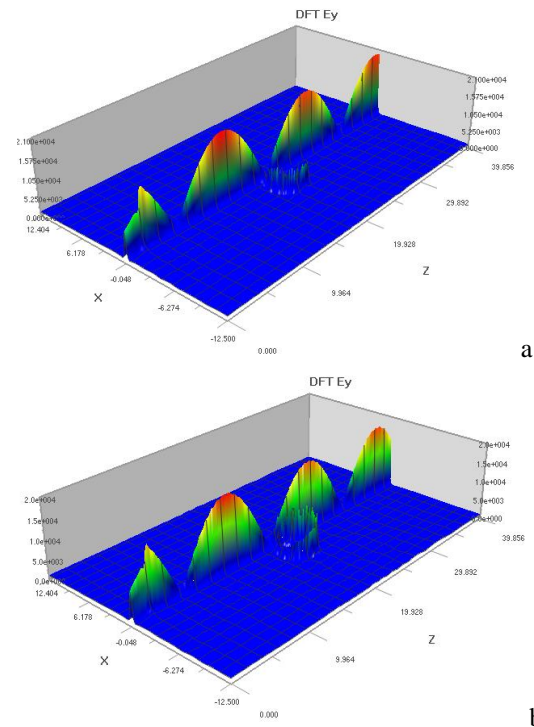


Fig. 6. The evolution of the E_y component of the field as function of the propagation distance for different pump powers and for two effective area $0,01 \mu\text{m}^2$ (a) and $0,09 \mu\text{m}^2$ (b)

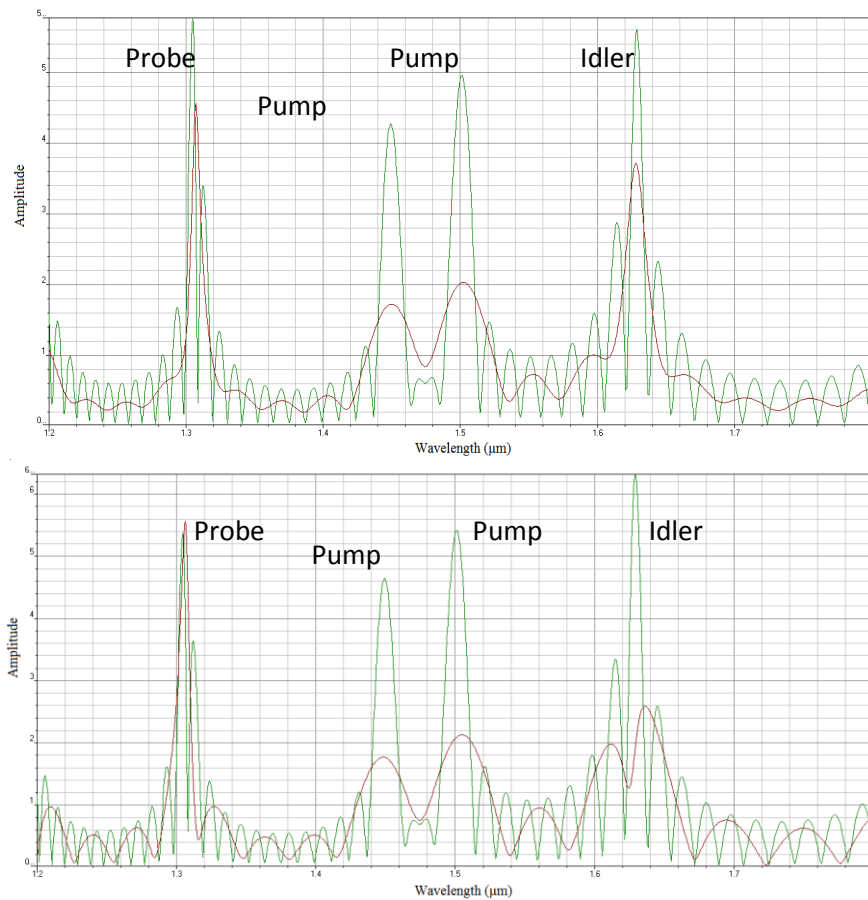


Fig. 7. The evolution of the optical field as function of wavelength for different pump powers and for two effective area $0,01 \mu\text{m}^2$ (up) and $0,09 \mu\text{m}^2$ (down)

4. Conclusions

In conclusion, by using CW pump we studied the nonlinear effects in a $40 \mu\text{m}$ SOI micro-ring resonator and we manage to photon pairs in these types of structures. The main advantage of these types of micro-rings is that can be used in long distances communication systems. Having in mind the future development in the field these types of structures can be integrated in quantum photonics circuits and might be used, in the future, in particle accelerating structures. In our FDTD based simulation we used different effective areas and different input wavelengths.

References

- [1] Jay E. Sharping, et al., Optics Express, 12388, **14**(25), (2006).
- [2] Laurent Olislager, et al., Optics Letters, **38**(11), 1960 (2013).
- [3] H. Takesue, et al., Appl. Phys. Lett., **91**, 201108 (2007).
- [4] H. Takesue, K. Inoue, Phys. Rev. **A70**, 031802(R), (2004).
- [5] Nobuyuki Matsuda, et al., Optics Express **21**, 8596 (2013).
- [6] Jingyun Fan, Matthew D. Eisaman, Alan Migdall,, Proc. of SPIE, **6780**, 67800Q (2007).
- [7] Q. Lin, G.P. Agrawal, Optics Letters, **31**(21), 2006.
- [8] K. Garay-Palmet, Optics Express, **15**(22), (2007).
- [9] <http://spectrum.ieee.org/semiconductors/devices/engineers-unveil-particle-accelerator-on-a-chip>
- [10] R.J. England, et al., Proceedings of Particle Accelerator Conference, New York, NY, USA, 2067-2070, 2011.
- [11] A. R. Sterian. "Advances in Optical Amplifiers", Paul Urquhart (Ed.), ISBN: 978-953-307-186-2, InTech, Vienna, 2011.
- [12] R.J. England, et al., Proceedings of Particle Accelerator Conference, New York, NY, USA, 346-348, 2011.
- [13] Z. Wu, C. Ng, C. McGuinness, E. Colby, Proceedings of Particle Accelerator Conference, New York, NY, USA, 241-243, 2011.

- [14] D. Alastair, et al., Proceedings of SPIE, Active and Passive Optical Components for WDM Communication IV, p. 359, 2004.
- [15] Ian M. White, Hesam Oveys, Xudong Fan, Optics Letters, **31**(9), (2006).
- [16] Yuze Sun & Xudong Fan, Anal Bioanal Chem., **399**, 205 (2011).
- [17] H. M. Hairi, et al., PIERS Proceedings, Xi'an, China, March 22-26, 2010.
- [18] E. Megidish, et al., <http://arxiv.org/abs/1209.4191>.
- [19] Pavel Sekatski, et al., Physical Review Letters **103**, 113601 (2009).
- [20] A. R. Sterian, Advances in High Energy Physics, Article Number: 839570, DOI: 10.1155/2013/839570, 2013.
- [21] D. Savastru, S. Dontu, et al., Advances in High Energy Physics, Article Number: 876870 DOI: 10.1155/2013/876870, 2013.
- [22] I. McGregor, K M Hock, Journal of Instrumentation, **8**, (2013).
- [23] Osamu Aso, Masateru Tadakuma, Shu Namiki, Furukawa Review, No. 19, 63 (2000).
- [24] Q. Lin, Oskar J. Painter, G. P. Agrawal, Optics Express, **15**(25), 16604 (2007).
- [25] A. R. Sterian, Hindawi Publishing Corporation, Advances in High Energy Physics, **2073**, Article ID 5 1 63 96, 8 pages, 2013.
- [26] D. Savastru, R. Savastru, S. Micloș, , I. Lancranjan, Journal of Ovonic Research, **9**(5), 147 (2013).
- [27] S. Miclos, D. Savastru, , I. Lancranjan, R. Savastru, C. Opran, (Conference Paper, PIERS 2013 Stockholm) Progress in Electromagnetics Research Symposium, 2013, Pages 48-51.
- [28] Allen Taflove, Susan C. Hagness, Computational Electrodynamics: The Finite-Difference Time-Domain Method, Second Edition, Artech House INC., London, 2000.
- [29] Andreea Fazacas, Paul Sterian, J. Optoelectron. Adv. Mater. **14**(3-4), 344 (2012).
- [30] http://www.optiwave.com/products/fdtd_overview.html
- [31] OptiFDTD Technical Background and Tutorials
- [32] S. Clemen, et al., "Continuous wave photon pair generation in silicon-on-insulator waveguides and ring resonators", <http://arxiv.org/pdf/0906.4688v1.pdf>
- [33] D. A. Anghel, et al., , Mathematical Problems in Engineering, Article Number: 736529 DOI: 10.1155/2012/736529, 2012.
- [34] R. Savastru, , I.I. Lancranjan, , D Savastru., S. Miclos, 10th Conference on Optics: Micro- to Nanophotonics III, ROMOPTO 2012; Bucharest, Romania; September 2013, Code 99208, Article number 88820Y, Volume 8882, 2013.
- [35] A.R. Sterian, P. Sterian, Mathematical Problems in Engineering, vol. 2012, Article ID 347674, 12 pages, doi:10.1155/2012/347674, 2012.
- [36] M. Ciobanu, et al., Journal of Computational and Theoretical Nanoscience, **10**(3), 705 (2013).
- [37] D. Savastru, , R. Savastru, , S. Miclos, I. Lancranjan, (Conference Paper, PIERS 2013 Stockholm) Progress in Electromagnetics Research Symposium, Pages 1776-1780, 2013.

*Corresponding author: a.fazacas@ifa-mg.ro